

SYNTHESIS, X-RAY CRYSTAL STRUCTURE, AND CATALYTIC EPOXIDATION PROPERTY OF AN OXOVANADIUM(V) COMPLEX WITH HYDRAZONE AND ETHYL MALTOL LIGANDS

Y. M. Cui^{1,2}, Y. Q. Wang², X. X. Su², H. Huang²,
and P. Zhang^{1*}

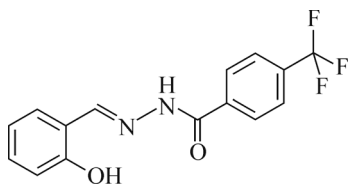
A new oxovanadium(V) complex [VO(BH)(EM)], where BH = *N'*-(2-hydroxybenzylidene)-4-trifluoromethylbenzohydrazide, EM = ethyl maltol, is synthesized and fully characterized based on the elemental analysis, FT-IR, UV-Vis, and ¹H NMR spectra. The complex is also characterized by single crystal X-ray diffraction, which indicates that the V atom adopts the octahedral coordination. The hydrazone ligand behaves as a tridentate ligand, and the ethyl maltol ligand behaves as a bidentate ligand. The catalytic epoxidation property of the complex is investigated.

DOI: 10.1134/S0022476619080092

Keywords: oxovanadium complex, hydrazone, ethyl maltol, X-ray crystal structure, catalytic epoxidation.

INTRODUCTION

Schiff bases are a kind of interesting ligands in coordination chemistry. Metal complexes with Schiff bases have attracted remarkable attention due to their facile synthesis and special biological, catalytic, and industrial applications [1-5]. Catalytic epoxidation of olefins is an important reaction in chemistry. Many transition metal complexes are active catalysts for this process [6-10]. However, among the complexes, vanadium ones seem to be more interesting because of their excellent catalytic ability in the oxidation of olefins and sulfides [11-13]. In this paper, a new vanadium(V) complex derived from *N'*-(2-hydroxybenzylidene)-4-trifluoromethylbenzohydrazide (BH, Scheme 1) and ethyl maltol (EM) is prepared and studied for its catalytic epoxidation property on cyclooctene.



Scheme 1. Hydrazone BH.

¹Engineering Research Center for Clean Production of Textile Printing and Dyeing, Ministry of Education, Wuhan Textile University, Wuhan, P. R. China; *zhping654321@163.com. ²School of Environmental Engineering, Wuhan Textile University, Wuhan, P. R. China. Original article submitted February 2, 2019; revised February 21, 2019; accepted March 15, 2019.

EXPERIMENTAL

Materials and methods. 4-Trifluoromethylbenzohydrazide was prepared as described in the literature [14]. Salicylaldehyde and VO(acac)₂ were purchased from Alfa Aesar and used as received. Reagent grade solvents were used as received. Microanalyses of the complexes were performed with a Vario EL III CHNOS elemental analyzer. Infrared spectra were recorded as KBr pellets with an FTS-40 spectrophotometer. Electronic spectra were recorded on a Lambda 900 spectrometer. ¹H NMR spectra were recorded on a Bruker spectrometer at 300 MHz. The catalytic reactions were followed by gas chromatography on an Agilent 6890A chromatograph equipped with an FID detector and a DB5-MS capillary column (30 m × 0.32 mm, 0.25 μm). Molar conductance measurements were made by means of a Metrohm 712 conductometer in acetonitrile.

Synthesis of the hydrazone compound BH. 4-Trifluoromethylbenzohydrazide (10 mmol, 2.04 g) and salicylaldehyde (10 mmol, 1.22 g) were refluxed in methanol (50 mL). The reaction was continued for 1 h in an oil bath during which a solid compound was separated. It was filtered and washed with cold methanol. The crude product was recrystallized from methanol and dried over anhydrous CaCl₂. Yield: 2.75 g (89%). IR data (KBr pellet, cm⁻¹): 3337 ν(O—H), 3223 ν(N—H), 1655 ν(C=O), 1613 ν(C=N). UV-Vis data in methanol (nm): 275, 350, 430. Analysis: found (%): C 58.31, H 3.72, N 9.23; calculated for C₁₅H₁₁F₃N₂O₂ (%): C 58.45, H 3.60, N 9.09. ¹H NMR (300 MHz, *d*⁶-DMSO): δ 12.26 (s, 1H, OH), 11.53 (s, 1H, NH), 8.72 (s, 1H, CH=N), 7.92 (d, 2H, ArH), 7.81 (d, 2H, ArH), 7.63 (d, 1H, ArH), 7.54 (t, 1H, ArH), 7.10-7.01 (m, 2H, ArH).

Synthesis of the [VO(BH)(EM)] complex. The hydrazone ligand (1.0 mmol, 0.31 g), ethyl maltol (1.0 mmol, 0.14 g), and VO(acac)₂ (1.0 mmol, 0.26 g) were refluxed in methanol (30 mL). The reaction was continued for 1 h in an oil bath to give a deep brown solution. Single crystals of the complex formed during slow evaporation of the reaction mixture in air. The crystals were isolated by filtration, washed with cold methanol, and dried over anhydrous CaCl₂. Yield: 0.29 g (57%). IR data (KBr pellet, cm⁻¹): 1607 ν(C=N), 1371 ν(C—O_{phenolate}), 1162 ν(N—N), 955 ν(V=O). UV-Vis data in acetonitrile (nm): 275, 320, 400. Molar conductance (10⁻³ M, acetonitrile): 20 Ω⁻¹·cm²·mol⁻¹. Analysis: found (%): C 51.30, H 3.27, N 5.61; calculated for C₂₂H₁₆F₃N₂O₆V (%): C 51.58, H 3.15, N 5.47. ¹H NMR (300 MHz, *d*⁶-DMSO): δ 9.26 (s, 1H, CH), 8.46 (s, 1H, CH=N), 8.06 (d, 2H, ArH), 7.85 (m, 3H, ArH), 7.60 (d, 1H, ArH), 7.10 (t, 1H, ArH), 6.90 (t, 1H, ArH), 6.70 (t, 1H, ArH), 3.02 (t, 3H, CH₂), 1.33 (s, 3H, CH₃).

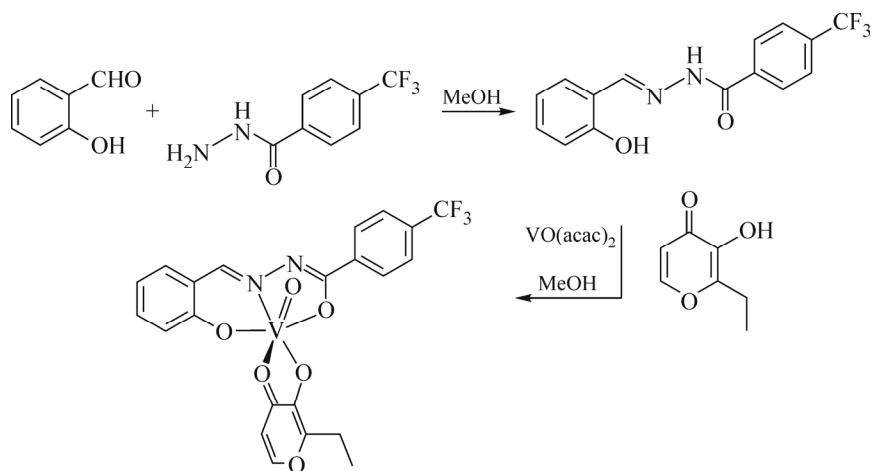
Crystal structure determination. Data were collected on a Bruker SMART 1000 CCD area diffractometer using a graphite monochromator and MoK_α radiation ($\lambda = 0.71073 \text{ \AA}$) at 298(2) K. The data were corrected with SADABS programs and refined on *F*² with the Siemens SHELXL software [15, 16]. The structure was solved by direct methods and difference Fourier syntheses. All non-hydrogen atoms were refined anisotropically. The hydrogen atoms were placed in calculated positions and included in the last cycles of the refinement. Crystal data and details of the data collection and refinement are listed in Table 1. Selected coordinate bond lengths and angles are listed in Table 2.

Catalytic epoxidation process. A mixture of cyclooctene (2.76 mL, 20 mmol), acetophenone (internal reference), and the complex as the catalyst (0.05 mmol) was stirred and heated up to 80 °C before the addition of aqueous *tert*-butyl hydroperoxide (TBHP; 70% w/w, 5.48 mL, 40 mmol). The mixture was initially an emulsion, but two phases became clearly visible as the reaction progressed (a colorless aqueous one and a yellowish organic one). The reaction was monitored for 5 h with the withdrawal and analysis of organic phase aliquots (0.1 mL) at required times. Each withdrawn sample was mixed with 2 mL of diethylether, treated with a small quantity of MnO₂, and then filtered through silica and analyzed by GC.

RESULTS AND DISCUSSION

Synthesis. The hydrazone compound and the complex were synthesized in a facile and analogous way (Scheme 2).

Hydrazone acts as a tridentate dianionic ONO donor ligand toward the VO³⁺ core. The oxovanadium complex was obtained from a refluxing mixture of hydrazone, ethyl maltol, and VO(acac)₂ in a 1:1 molar proportion in methanol. The



Scheme 2. Synthesis of hydrazone and the complex.

TABLE 1. Crystallographic Data for the Complex

Parameters	Values
Empirical formula	C ₂₂ H ₁₆ F ₃ N ₂ O ₆ V
Formula weight	512.31
Crystal size, mm	0.30×0.30×0.28
Crystal system	Triclinic
Space group	P1
<i>a</i> , <i>b</i> , <i>c</i> , Å	10.153(2), 10.790(2), 11.320(2)
α, β, γ, deg	114.884(2), 92.435(2), 94.069(2)
<i>V</i> , Å ³	1118.5(3)
<i>Z</i>	2
ρ _{calc} , g/cm ³	1.521
μ, mm ⁻¹	0.510
<i>F</i> (000)	520
θ range for data collection, deg	2.72-25.50
Index ranges	-12 ≤ <i>h</i> ≤ 12, -13 ≤ <i>k</i> ≤ 11, -13 ≤ <i>l</i> ≤ 13
Measured / Independent reflections	10072 / 4082
Observed reflections (<i>I</i> > 2σ(<i>I</i>))	3465
Parameters	308
Restraints	0
Data completeness	0.981
Maximum and minimum transmission	0.8621 and 0.8704
Final <i>R</i> indices [<i>I</i> > 2σ(<i>I</i>)]	0.0567, 0.1552
<i>R</i> indices (all data)	0.0667, 0.1668
GOOF on <i>F</i> ²	1.067
Largest difference in peak and hole, e/Å ³	0.771 and -0.619

complex was isolated as brown single crystals from the reaction mixture by slow evaporation at room temperature. Crystals of the complex are stable at room temperature and are found to be fairly soluble in most common organic solvents such as methanol, ethanol, acetonitrile, DMF, and DMSO. The low molar solution conductance of the complex in acetonitrile indicates its non-electrolyte behavior.

IR and electronic spectra. The IR spectrum of hydrazone shows bands centered at 3223 cm^{-1} for $\nu(\text{N}-\text{H})$, 3337 cm^{-1} for $\nu(\text{O}-\text{H})$, and 1655 cm^{-1} for $\nu(\text{C}=\text{O})$ [17, 18]. The peaks attributed to $\nu(\text{N}-\text{H})$ and $\nu(\text{C}=\text{O})$ are absent in the spectrum of the complex as the ligand binds in the dianionic form, resulting in losing a proton from the carbohydrazide group. A strong band observed at 1607 cm^{-1} for the complex is attributed to $\nu(\text{C}=\text{N})$, which is located at lower frequencies as compared to the free hydrazone ligand, *viz.* 1613 cm^{-1} [19, 20]. The complex exhibits a characteristic band at 955 cm^{-1} for the stretching of the $\text{V}=\text{O}$ bond [21]. Based on the IR absorption, it is obvious that the hydrazone ligand exists in the uncoordinated form in the *keto*-amino tautomer and in the complex in the imino-enol tautomeric form. This is not uncommon in the coordination of hydrazone compounds [22-24].

The electronic spectrum of the complex recorded in acetonitrile displays a strong absorption band centered at 400 nm , which is assigned as charge transfer transitions of $\text{N}(p\pi)-\text{Mo}(d\pi)$ LMCT. The medium absorption band centered at 320 nm is assigned as charge transfer transitions of $\text{O}(p\pi)-\text{Mo}(d\pi)$ LMCT [25, 26].

Description of the structure of the complex. The perspective view of the complex together with the atom numbering scheme is shown in Fig. 1. The coordination geometry around the V atom reveals a distorted octahedral environment with the NO_5 chromophore. The hydrazone ligand behaves as a dianionic tridentate ligand binding through

TABLE 2. Selected Bond Lengths (\AA) and Angles (deg) for the Complex

V1–O1	1.839(2)	V1–O2	1.926(2)
V1–O3	2.294(2)	V1–O4	1.864(2)
V1–O6	1.578(2)	V1–N1	2.087(2)
O6–V1–O1	100.22(13)	O6–V1–O4	98.70(11)
O1–V1–O4	105.22(10)	O6–V1–O2	98.85(12)
O1–V1–O2	153.46(11)	O4–V1–O2	89.89(9)
O6–V1–N1	98.27(11)	O1–V1–N1	84.26(10)
O4–V1–N1	158.71(10)	O2–V1–N1	74.85(9)
O6–V1–O3	175.64(11)	O1–V1–O3	82.23(10)
O4–V1–O3	77.12(8)	O2–V1–O3	80.02(9)
N1–V1–O3	85.53(9)		

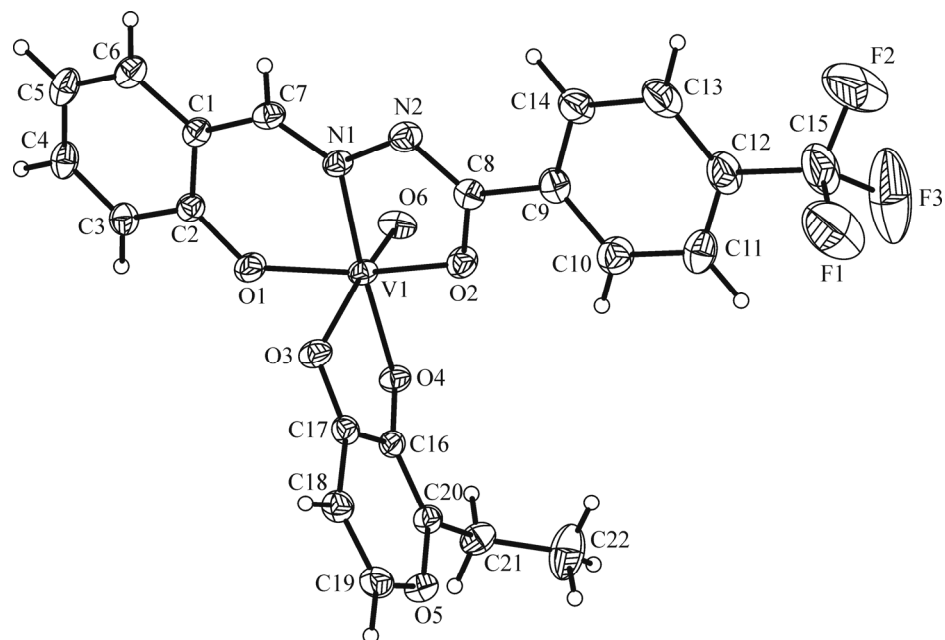


Fig. 1. ORTEP plots (30% probability level) and numbering scheme for the complex.

phenolate oxygen, enolate oxygen, and imine nitrogen atoms, and occupies three positions in the equatorial plane. The fourth position of the equatorial plane is occupied by the hydroxyl group of the ethyl maltol ligand. The carbonyl oxygen atom of the ethyl maltol ligand occupies one axial position of the octahedral coordination, and another axial position is occupied by the oxo group. The vanadium atom is found to deviate from the mean equatorial planes defined by the four donor atoms by 0.301(1) Å. The V1–O3 bond length is longer than the normal single bond lengths (2.29 Å against 1.9–2.0 Å). This shows that the carbonyl oxygen atom is loosely attached to the V center. The remaining V–O and V–N bond lengths are similar to other vanadium(V) complexes [27, 28]. The C8–O2 bond length in the complex is 1.31 Å, which is closer to single bond length rather than C=O double bond length. However, the shorter length compared to the C–O single bond may be attributed to the extended electron delocalization in the ligand [26]. A similar shortening of the C8–N2 bond length (1.29 Å instead of normal 1.38 Å) together with the elongation of the N1–N2 bond length (1.40 Å) also supports the electron cloud delocalization in the ligand system. The hydrazone ligand forms five- and six-membered chelate rings with the V center. The five-membered metallacycle is quite planar, but the six-membered metallacycle is clearly distorted. The dihedral angle between the two benzene rings is 4.0(3)°. The *trans* angles are in the range 153.46(11)–175.64(11)°, indicating a considerable distortion of the coordination octahedron around the V center.

The crystal packing diagram of the complex is shown in Fig. 2. The adjacent complex molecules are linked by $\pi \cdots \pi$ stacking interactions (Table 3).

Catalytic epoxidation results. Before the addition of aqueous TBHP at 80 °C, the complex dissolved completely in the organic phase. The aqueous phase of the solution was colorless and the organic phase was brown, indicating that the catalyst is mainly confined in the organic phase. TBHP is mainly transferred into the organic phase under those conditions,

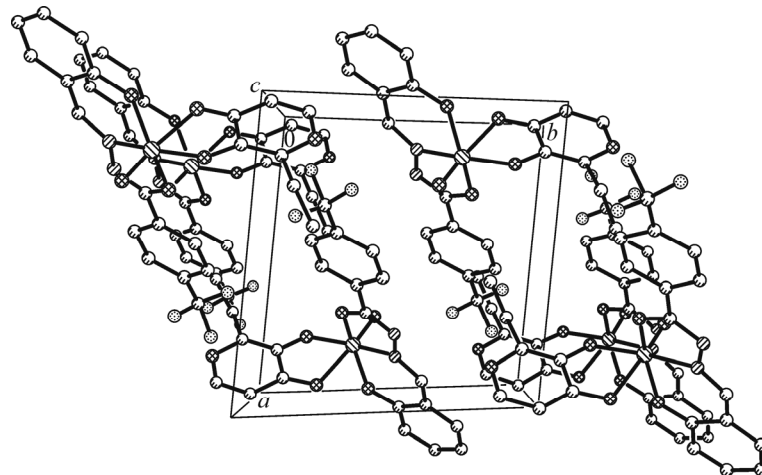


Fig. 2. Molecular packing diagram of the complex, viewed down the *c* axis.

TABLE 3. $\pi \cdots \pi$ Stacking Interactions of the Complex

$Cg(I) \cdots Cg(J)$	d (Å)	$Cg(I) \cdots Cg(J)$	d (Å)
$Cg(1) \cdots Cg(2)$	2.767(3)	$Cg(1) \cdots Cg(3)$	4.682(3)
$Cg(1) \cdots Cg(4)^{\#1}$	4.798(3)	$Cg(1) \cdots Cg(5)^{\#2}$	4.361(3)
$Cg(1) \cdots Cg(2)^{\#3}$	4.944(3)	$Cg(2) \cdots Cg(3)^{\#3}$	3.709(3)
$Cg(3) \cdots Cg(3)^{\#3}$	3.572(3)	$Cg(4) \cdots Cg(3)^{\#4}$	4.963(3)
$Cg(4) \cdots Cg(5)^{\#1}$	3.973(3)		

Symmetry codes: ^{#1} 2–*x*, 1–*y*, 1–*z*; ^{#2} 1–*x*, 1–*y*, 1–*z*; ^{#3} 2–*x*, –*y*, –*z*; ^{#4} *x*, 1+*y*, *z*.

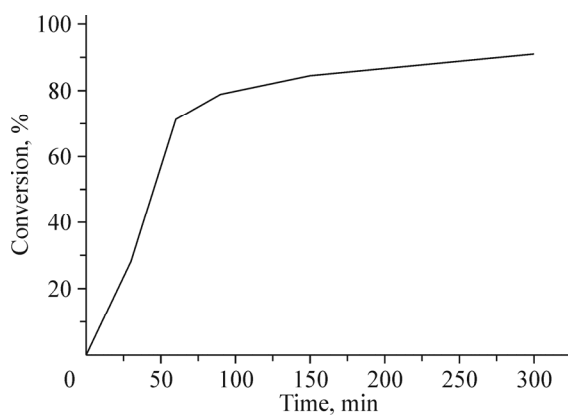
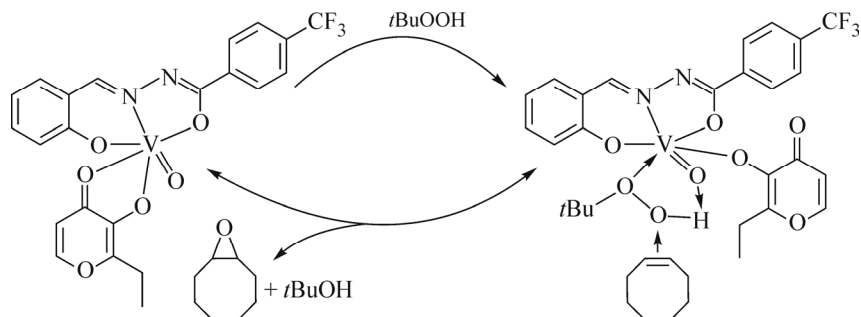


Fig. 3. Kinetic monitoring of *cis*-cyclooctene epoxidation with TBHP–H₂O in the presence of the complex.

and for that reason the reactant and products in the organic layer were analyzed. Cyclooctene and cyclooctene oxide are not significantly soluble in water, therefore the determination of the epoxide selectivity (epoxide formation/cyclooctene conversion) is expected to be accurate. As for the cyclooctene epoxidation with aqueous TBHP, with no extra addition of organic solvents, the present study shows the effective activity. Kinetic profiles of the complex as the catalyst are presented in Fig. 3. No induction time was observed. The cyclooctene conversion for the complex is 91% after 5 h, and the selectivity towards cyclooctene oxide is 61%. A possible mechanistic consideration involves the coordination of TBHP as a neutral molecule, with the O–H···O hydrogen bond (Scheme 3).



Scheme 3. Proposed mechanism for the catalytic process of the complex.

CONCLUSIONS

In summary, a new oxovanadium(V) complex with tridentate hydrazone and ethyl maltol ligands has been synthesized and characterized. The V atom of the complex is in the octahedral coordination. The complex can catalyze the epoxidation of cyclooctene with a high conversion.

FUNDING

This work was supported by the Collaborative Innovation Plan of Hubei Province for Key Technology of Eco-Ramie Industry.

ADDITIONAL INFORMATION

CCDC number 1824512 contains the supplementary crystallographic data for the complex. These data can be obtained free of charge *via* <http://www.ccdc.cam.ac.uk/conts/retrieving.html>, or from the Cambridge Crystallographic Data Center, 12, Union Road, Cambridge CB2 1EZ, UK; fax: +44 1223 336 033; or e-mail: deposit@ccdc.cam.ac.uk.

CONFLICT OF INTERESTS

The authors declare that they have no conflict of interests.

REFERENCES

1. M. C. Heffern, V. Reichova, J. L. Coomes et al. *Inorg. Chem.*, **2015**, *54*(18), 9066–9074.
2. S. Meghdadi, M. Amirnasr, M. Majedi et al. *Inorg. Chim. Acta*, **2015**, *437*, 64–69.
3. D. Qu, F. Niu, X. Zhao et al. *Bioorg. Med. Chem.*, **2015**, *23*(9), 1944–1949.
4. H. Zafar, A. Ahmad, A. U. Khan et al. *J. Mol. Struct.*, **2015**, *1097*, 129–135.
5. X. Zhao, X. Chen, J. Li et al. *Polyhedron*, **2015**, *97*, 268–272.
6. R. G. Mohamed, F. M. Elantabli, N. H. Helal et al. *Synth. React. Inorg. Met.-Org. Nano-Met. Chem.*, **2015**, *45*(12), 1839–1850.
7. T. S. M. Oliveira, A. C. Gomes, A. D. Lopes et al. *Dalton Trans.*, **2015**, *44*(31), 14139–14148.
8. C. A. Koellner, N. A. Piro, W. S. Kassel et al. *Inorg. Chem.*, **2015**, *54*(15), 7139–7141.
9. T. Alemohammad, N. Safari, S. Rayati et al. *Inorg. Chim. Acta*, **2015**, *434*, 198–208.
10. M. Bagherzadeh, A. Ghanbarpour, and H. R. Khavasi. *Catal. Commun.*, **2015**, *65*, 72–75.
11. H. Y. Liu, L. Q. Zang, and J. L. Lv. *Russ. J. Coord. Chem.*, **2015**, *41*, 451–455.
12. S. Morales-delaRosa, J. M. Campos-Martin, P. Terreros et al. *Topics Catal.*, **2015**, *58*(4–6), 325–333.
13. T. Baskaran, R. Kumaravel, J. Christopher et al. *New J. Chem.*, **2015**, *39*(5), 3758–3764.
14. M. Amir and K. Shikha. *Eur. J. Med. Chem.*, **2004**, *39*, 535–545.
15. G. M. Sheldrick. SADABS. Siemens Analytical X-ray Instrument Division: Madison, WI, 1995.
16. G.M. Sheldrick. SHELXS97 Program for Solution of Crystal Structures. University of Göttingen, Germany, 1997.
17. Y.-T. Ye, F. Niu, Y. Sun et al. *Chinese J. Inorg. Chem.*, **2015**, *31*(5), 1019–1026.
18. Z.-L. You, D.-M. Xian, and M. Zhang. *CrystEngComm*, **2012**, *14*(21), 7133–7136.
19. R. A. Lal, M. Chakrabarty, S. Choudhury et al. *J. Coord. Chem.*, **2010**, *63*(1), 163–175.
20. T. Glowiacz, L. Jerzykiewicz, J. M. Sobczak et al. *Inorg. Chim. Acta*, **2003**, *356*, 387–392.
21. C. A. Koellner, N. A. Piro, W. S. Kassel et al. *Inorg. Chem.*, **2015**, *54*(15), 7139–7141.
22. L.-X. Li, Y. Sun, Q. Xie et al. *Chinese J. Inorg. Chem.*, **2016**, *32*(2), 369–376.
23. L. Pan, C. Wang, K. Yan et al. *J. Inorg. Biochem.*, **2016**, *159*(1), 22–28.
24. D. Qu, F. Niu, X. Zhao et al. *Bioorg. Med. Chem.*, **2015**, *23*(9), 1944–1949.
25. R. Hahn, U. Kusthardt, and W. Scherer. *Inorg. Chim. Acta*, **1993**, *210*(2), 177–182.
26. S. Gupta, A. K. Barik, S. Pal et al. *Polyhedron*, **2007**, *26*(1), 133–141.
27. M. R. Maurya, S. Agarwal, C. Bader et al. *Dalton Trans.*, **2005**, *(3)*, 537–544.
28. H. H. Monfared, S. Alavi, R. Bikas et al. *Polyhedron*, **2010**, *29*(18), 3355–3362.